

Jonathan D. Burns¹ and Bruce A. Moyer²

¹Nuclear Security Science & Policy Institute, Department of Nuclear Engineering,
Texas A&M University, College Station, TX 77845, USA

²Chemical Sciences Division,
Oak Ridge National Laboratory, P.O. Box 2008, Oak Ridge, TN 37831

For submission to publish in the
Journal of Cleaner Production
as a full-length article.

Uranyl nitrate hexahydrate solubility in nitric acid and its crystallization selectivity in the presence of nitrate salts

This submitted manuscript has been authored by Texas A&M University under Subcontract No. 4000147738 with UT-Battelle, LLC, under Contract No. DE-AC0500OR22725 with the U.S. Department of Energy. The United States Government retains and the publisher, by accepting the article for publication, acknowledges that the United States Government retains a non-exclusive, paid-up, irrevocable, world-wide license to publish or reproduce the published form of this manuscript, or allow others to do so, for the United States Government purposes. *The Department of Energy will provide public access to these results of federally sponsored research in accordance with the DOE Public Access Plan (<http://energy.gov/downloads/doe-public-access-plan>).*

Research sponsored by the Fuel Cycle Research and Development program, Office of Nuclear Energy, U.S. Department of Energy.

Uranyl nitrate hexahydrate solubility in nitric acid and its crystallization selectivity in the presence of nitrate salts

Jonathan D. Burns^{*,a} and Bruce A. Moyer^b

^aNuclear Science Security & Policy Institute, Texas A&M University, College Station, TX 77845, USA

^bChemical Sciences Division, Oak Ridge National Laboratory, PO Box 2008, Oak Ridge, TN 37831, USA

ABSTRACT:

The solubility of uranyl nitrate hexahydrate was determined as a function of nitric acid concentration and temperature, and the crystallization yield was calculated. Results showed an increase in crystal formation at lower initial nitric acid concentrations upon cooling a saturated solution of U(VI) from 50 °C to 2 °C, with over 70% recovery of U(VI) mass at all nitric acid concentrations and nearly quantitative recovery starting at 4 M HNO₃. A direct correlation between the change in mother liquor volume percent and U mass removal percent was observed. By reducing the cooling rate from roughly 4.0 °C/min to 0.22 °C/min, the separation factor was increased from 3.88–15.7 to greater than 81 for the separation of U(VI) from Sr, Cs, and Nd. At the slower cooling rate, the separation factors were measured as a function of acidity for 2.0–4.3 M HNO₃, showing a decrease in selectivity with a decrease in the acidity. There was also no indication that tetravalent metal double-salt precipitation occurred with either Zr⁴⁺ or Ce⁴⁺. These results indicate that a high-yield, high purity hexavalent actinide crystallization scheme may offer attractive benefits for nuclear-fuel recycle in that only a single very simple and well-understood technology is employed, and the use of organic compounds and solvents is avoided.

1. Introduction

A comprehensive, forward-thinking sustainable energy strategy is thought to include nuclear power as a base-load component in its portfolio; however, nuclear power must get around several obstacles to reap the benefits of its intrinsic carbon-free power generation, diminishing concerns around greenhouse gas emissions.(Grimes and Nuttall, 2010; Kharecha and Hansen, 2013; Sailor, 2000) A challenging barrier to overcome entails the separations involved in the recycle of used fuel aimed at recovering the actinides (Ans) to maximize energy utilization of the fuel while keeping the heat-generating and radiotoxic waste going to geologic storage at a minimum without neglecting concerns around nonproliferation.(Grimes and Nuttall, 2010; Kharecha and Hansen, 2013; Sailor, 2000) The most advanced technologies target recovery of U and Pu to preserve key energy-generating components, as well as the minor Ans (MAs, i.e., Np, Am, and Cm), which are the most detrimental when considering the heat load and long-term hazards of

geologic disposal(Poinssot et al., 2015; Salvatores and Palmiotti, 2011; Tachimori and Morita, 2009; Todd and Wigeland, 2006; Wigeland et al., 2006). Although recent progress has led to viable separation processes, they suffer from complexity accompanied by significant costs.(Wigeland et al., 2015) Much effort to achieve sufficient separations has focused on solvent extraction(Ansari et al., 2011; Manchanda et al., 2009) and to a lesser extent ion exchange(Burns et al., 2012a, 2012b, 2012c). A compelling tactic to this problem would be to produce a single-step technology, which would separate all the actinides at once. This approach is known as a Group ActiNide EXtraction (GANEX) type process.(Aneheim et al., 2010; Miguiditchian et al., 2007) In one type of GANEX strategy, a highly oxidizing environment must be created and maintained to stabilize the resulting hexavalent states long enough to perform the separation. With the reduction potentials of Am(VI)/Am(III) being on the order of +1.7 V vs NHE(Runde and Mincher, 2011), Am(VI) becomes the most problematic to oxidize and stabilize. Methods for achieving the oxidation are challenging and under intense investigation.(Burns et al., 2012b, 2012c; Dares et al., 2015; Grimes and Mincher, 2015; Mincher et al., 2015a, 2015b, 2012, 2008) Of the different methods being explored, oxidation using sodium bismuthate has been shown by Mincher et al.(Mincher et al., 2015a, 2015b, 2012, 2008; Moyer et al., 2015; Runde and Mincher, 2011) to be an effective chemical oxidant for Am(III), though it suffers from slow kinetics and adds significant new mass to the resulting waste stream.

Inspired by this GANEX-type separation concept, we have recently purposed and demonstrated a hexavalent actinide co-crystallization separation, where U through Am could be separated as crystalline nitrate salts.(Burns and Moyer, 2016) The hexavalent actinides were shown to be removed from solution in near proportion to one another as uranyl nitrate hexahydrate (UNH) crystallized out of solution, whereas the lower valent actinides, tri- and tetravalent, were only slightly removed from solution. Separation factors of 7–70 were observed for Zr, Cs, and Ce. While our previous work demonstrated that, once oxidized, the hexavalent actinides can indeed all be co-crystallized together and a separation from fission products is possible, the studies were limited to proof-of-concept. No attempt was made to maximize the recovery of An(VI) species or improve the selectivity of the process during these proof-of-concept studies, leaving important questions unanswered surrounding yield and selectivity for the An(VI) species by crystallization. In this work, we systematically investigate the yield and selectivity of the An(VI) crystallization process, aiming to show high recovery while rejecting key fission products.

2. Experimental

2.1 Materials

Nitric acid (69–70% Omni Trace, HNO₃) was purchased from EDM; cerium(III) nitrate hexahydrate (99.5%, Ce(NO₃)₃•6H₂O), cesium nitrate (99.8%, CsNO₃), neodymium(III) nitrate hydrate (99.99%, Nd(NO₃)₃•*n*H₂O), sodium bismuthate (ACS Grade, NaBiO₃), strontium nitrate

(99.0%, $\text{Sr}(\text{NO}_3)_2$), and zirconyl chloride octahydrate (98%, $\text{ZrOCl}_2 \cdot 8\text{H}_2\text{O}$) were all purchased from Alfa Aesar; depleted uranyl nitrate hexahydrate (ACS Grade, $\text{UO}_2(\text{NO}_3)_2 \cdot 6\text{H}_2\text{O}$) was purchased from SPI Supplies, and all were used as received. Deionized (DI) H_2O was obtained from an ELGA LabWater Purelab Flex ultrapure laboratory water purification system operated at 18.2 $\text{M}\Omega$ cm at 25 °C.

2.2 Solubility of UNH

Small batch crystallization experiments of 700–1100 μL volumes of an initial U concentration of 3.0–5.5 M and acidity of 4.0–8.5 N at 50 °C were conducted (see SI for experimental details). The system was temperature controlled in a water-jacketed sand bath using a temperature-controlled VWR® Refrigerated Circulating Bath Model MX7LL R-20 with a VWR digital temperature controller. The batches were progressively cooled to ≤ 2 °C in ~ 10 °C increments, and the phases were separated by decantation, whereupon the U concentration in the liquid phase was determined by inductively-coupled plasma mass spectrometry (ICP-MS) with a Perkin Elmer NexION 300D ICP-MS. Separating the phases at each 10 °C interval prevented larger amounts of the liquid phase to be trapped within the solid phase.

2.3 Crystallization Selectivity

Small batch crystallization experiments of 260–340 μL volumes were performed with $\text{UO}_2(\text{NO}_3)_2 \cdot 6\text{H}_2\text{O}$ as the desired product (see SI for experimental details). The initial U(VI) concentrations ranged from 3.4–4.3 M, while other metals, simulating key fission products Sr, Cs, and Nd were present at concentrations of 6–32 mM, 20–48 mM, 24–70 mM, respectively, and roughly 120 mM NaBiO_3 , if present, at an acidity ranging from 2.0–4.5 N. The experiments investigating double nitrate salt formation of tetravalent ions with Cs were conducted in a similar fashion, with 310–330 μL volumes, with the initial U(VI) concentrations ranging from 3.5–3.9 M and either 27 mM and 14 mM concentration of Cs and Zr, respectively, or 29 mM and 14 mM concentration of Cs and Ce, respectively, with an acidity of 4.4 M HNO_3 . In the case of the Cs-Ce system, approximately 120 mM NaBiO_3 was present to ensure the existence of Ce^{4+} . The systems were first heated to ca. 58 °C and then cooled to 18 °C in a water-jacketed sand bath as described above. After crystallization, the solid and liquid phases were separated by centrifugation with a Costar® Spin-X® 0.45 μm cellulose acetate centrifuge tube filter with a mini-centrifuge. The solutions were analyzed before and after crystallization by ICP-MS to determine the metal concentrations changes as a result of crystallization.

3. Results and Discussion

3.1 Solubility of UNH

The solubility of UNH was studied at 50 °C as a function of initial nitric acid concentration in the range 4.0–8.5 N as shown in Table 1. The UNH solubility decreased as the nitric acid concentration increased, as expected by Equation (1). An increase in nitrate concentration will shift the equilibrium to the right, reducing the amount of U(VI) in solution. This decrease in solubility at higher nitric acid concentration is advantageous and will be discussed further below.

Table 1: Solubility of uranyl nitrate at 50 °C with different initial nitric acid concentrations.

| [HNO ₃] (M) | [U(VI)] (M) | [U(VI)] (g/L) |
|-------------------------|-------------|---------------|
| 4.0 ± 0.1 | 3.8 ± 0.1 | 910 ± 30 |
| 5.8 ± 0.2 | 3.4 ± 0.1 | 800 ± 20 |
| 7.7 ± 0.3 | 3.5 ± 0.1 | 840 ± 30 |
| 8.5 ± 0.3 | 2.6 ± 0.1 | 610 ± 20 |



The system was then cooled in 10 °C increments, allowing UNH to crystallize out of solution. Figure 1 displays the U(VI) concentration in solution for the four systems at each temperature. The system with the initial nitric acid concentration of 4.0 ± 0.1 M was observed to have the largest difference in U(VI) concentration upon reducing the temperature from 50 °C down to 2 °C, and this difference decreases with an increase in initial nitric acid concentration. These results indicate that a lower initial nitric acid concentration will result in a higher crystallization yield. As shown in Table 2, the crystallization yields were observed to be ≥70% in all cases upon cooling to ≤2 °C. Most notably, when the initial nitric acid concentration was set to 4 M, a crystallization yield of over 90% was observed even at room temperature (20 °C), eliminating the burden of the energy-intensive process of cooling.

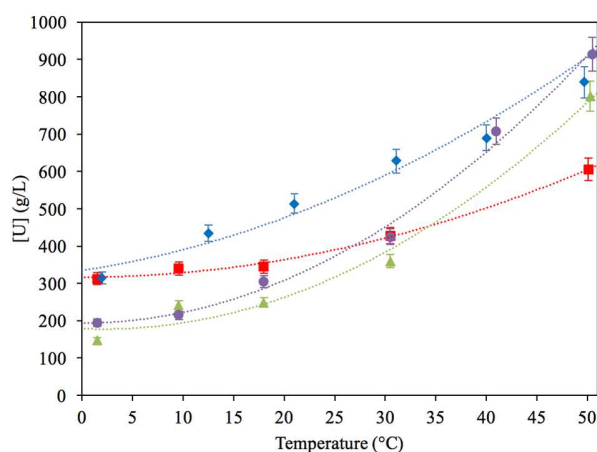


Figure 1: Uranium solubility limit as a function of temperature with an initial nitric acid concentration of 8.5 M (■), 7.7 M (◆), 5.8 M (▲) and 4.0 M (●) at 50 °C, dotted line for visual aid.

The major contributing factor to these high yields is the significant reduction in solution volume as the UNH is being removed from solution (see Table 3). This relationship can be seen clearly

by plotting the supernate percent volume relative to the initial volume verse the percent U mass removed from solution, as shown in Figure 2 (see SI for regression parameter statistics). There is a linear relationship between the slopes in Figure 2 and the initial acidity that can be written as follows ($R^2 = 0.996$):

$$\frac{\frac{V_f}{V_I}}{\frac{m_I - m_f}{m_I}} = 6.83 \times 10^{-2} \frac{L}{mol} \times [HNO_3]_f - 1.08 \quad (2)$$

where V equals the volume of the solution, m equals the mass of U.

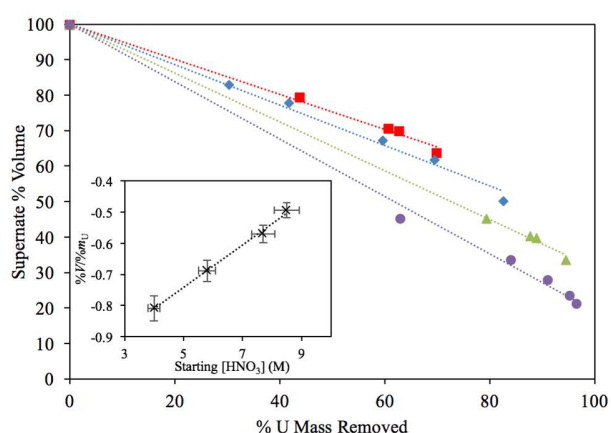


Figure 2: Relationship of supernate percent volume relative to the initial volume verse the percent U mass removed from solution with an initial nitric acid concentration of 8.5 M (■), 7.7 M (◆), 5.8 M (▲) and 4.0 M (●) at 50 °C, dotted linear fit. Inset displays the $\%V/\%m_U$ verse nitric acid concentration.

Assuming all the free protons stay in solution, the overall acidity of the mother liquor will increase as the crystallization progresses. The solubility of U(VI) is known to decrease as the nitric acid concentration increases, reaching a minimum between 6–8 M HNO_3 , with a slight increase as the nitric acid increases further. (*Nuclear Fuel Recovery and Recycling Center. License application, PSAR, volume 7, 1976*) The reduction of volume and the solubility of U(VI) as a function of nitric acid concentration provide an advantageous situation for a U recovery method based on UNH crystallization. That is to say, by starting in an environment favorable for dissolution with a high solubility limit (low acidity) and simply reducing the temperature of the system, forcing crystallization to initiate, maximizes crystallization with a low solubility limit by increasing the acidity of the mother liquor. This could further be improved upon by increasing the initial temperature closer to 60 °C; however, caution must be taken as the melting point of UNH is 60 °C, (Haynes, 2016) and thus temperatures ≥ 60 °C may cause too-rapid solid-phase formation upon cooling, which is unfavorable for a selective separation process based on crystallization. This will be discussed further below.

Nakahara *et al.* (Nakahara *et al.*, 2013) attributed the decrease in the mother liquor volume to the removal of water molecules from solution into the crystalline lattice; however, in the case where the initial nitric acid concentration was set to 4 M, roughly 7.69 mmol of H₂O was calculated to be removed in the form of UNH. In solution, 7.69 mmol of H₂O should occupy approximately 138 μ L of volume. The actual volume change was measured to be 630 ± 20 μ L, a factor of 4.6 greater than the calculated contribution due to water removal. Similar values result by performing the same arithmetic in the other three cases. It is our belief, that the major contributor to the decrease in volume is the uranium itself, which also dominates the total mass of the system.

Table 2: Percent mass recovery of U(VI) as UNH crystallizing out of solution.

| [HNO ₃] (M) | % U mass Recovery | | | | | |
|----------------------------|-------------------|------------|------------|------------|------------|------------|
| | 50 °C | 40 °C | 30 °C | 20 °C | 10 °C | 2 °C |
| 8.5 \pm 0.3 | 0 | - | 44 \pm 1 | 61 \pm 2 | 63 \pm 2 | 70 \pm 2 |
| 7.7 \pm 0.3 | 0 | 30 \pm 1 | 42 \pm 1 | 60 \pm 2 | 70 \pm 2 | 83 \pm 2 |
| 5.8 \pm 0.2 | 0 | - | 79 \pm 2 | 88 \pm 3 | 89 \pm 3 | 95 \pm 3 |
| 4.0 \pm 0.1 | 0 | 63 \pm 2 | 84 \pm 3 | 91 \pm 3 | 95 \pm 3 | 97 \pm 3 |

Table 3: Reduction in mother liquor volume upon decrease in temperature resulting in UNH crystal formation

| [HNO ₃] (M) | % Volume of Mother Liquor | | | | | |
|----------------------------|---------------------------|------------|------------|------------|------------|------------|
| | 50 °C | 40 °C | 30 °C | 20 °C | 10 °C | 2 °C |
| 8.5 \pm 0.3 | 100 | - | 79 \pm 2 | 71 \pm 2 | 70 \pm 2 | 64 \pm 2 |
| 7.7 \pm 0.3 | 100 | 83 \pm 2 | 78 \pm 2 | 67 \pm 2 | 62 \pm 2 | 50 \pm 1 |
| 5.8 \pm 0.2 | 100 | - | 45 \pm 1 | 40 \pm 1 | 40 \pm 1 | 34 \pm 1 |
| 4.0 \pm 0.1 | 100 | 45 \pm 1 | 34 \pm 1 | 28 \pm 1 | 23 \pm 1 | 21 \pm 1 |

3.2 Separation Selectivity

As the primary interest of this research is to achieve a group separation of the hexavalent actinides from fission products, it is important to understand how the other species will behave, particularly key fission products like Sr, Cs, and Nd. To begin with, the rate at which the system was cooled was examined. Table 4 shows the result of changing the rate of cooling from 58 °C to 18 °C from ≥ 4.0 °C/min to ≤ 0.22 °C/min. The slower cooling rate was shown to have a significant impact and be much more selective, producing an improved separation.

When the rate of cooling was reduced to ≤ 0.22 °C/min the selectivity of the An(VI) species was significantly enhanced. This is most obvious when considering Sr, which resulted in a greater than 20-fold improvement from the faster cooling rate to the slower cooling rate, while the other two fission product species, Cs and Nd, had slightly less significant enhancements, showing only a five-fold improvement. This was expected, as a slowing cooling rate will also reduce the rate at which the crystal formation and growth occurs. Slower crystal formation, allows nucleation to occur at the solubility limit, rather than forming a supersaturated solution. In a supersaturated solution precipitous crystallization can occur, trapping impurities within the crystalline phase.

Slow crystal growth also reduces the number of defects within the lattice, whereas with rapid crystal growth there is opportunity for defects in the structure to occur, which could include incorporation of contaminate species. The slight difference in UNH yield observed in this experiment is believed not to be caused by the cooling rate, but rather by the slight increase in HNO₃ concentration of 4.5 M for the faster rate to that of 4.3 M HNO₃ in the slower rate.

Table 4: Selectivity at different cooling rate. Acidity at 4.5 M and 4.3 M HNO₃ for 4.0 °C/min and 0.22 °C/min, respectively.

| Analyte | 4.0 °C/min | | 0.22 °C/min | |
|------------------|-------------|-------|-------------|-------|
| | %Removed | %U/%M | %Removed | %U/%M |
| Sr ²⁺ | 20% ± 1% | 3.88 | <1% | >81 |
| Cs ⁺ | 5.0% ± 0.3% | 15.7 | <1% | >81 |
| Nd ³⁺ | 5.0% ± 0.3% | 14.5 | <1% | >81 |
| U(VI) | 78% ± 4% | - | 81% ± 4% | - |

Next, the nitric acid shown to affect selectivity of the separation, where dilution the system below 4.3 M HNO₃ negatively impacted the selectivity. For this the separation was determined as a function of nitric acid concentration upon cooling the system from 58 °C down to 18 °C at the slower rate (Table 5). At the initial acidity of 4.3 M HNO₃, the contaminant fission products are quantitatively left in the mother liquor supernate after crystallization, with roughly 81% of U(VI) recovered from solution, as seen earlier. Decreasing the initial acidity to 3.4 M increase the overall removal of U(VI) to approximately 84%, but also caused some of the Sr to be removed from solution as well, ca. 58%, and therefore reducing the separation factor. The slight increase in separation factor at 3.4 M for Cs and Nd up to >84 is an artifact of more U(VI) being recovered from solution. Selectivity decreased to an even greater extent when the initial acidity was decrease further to 2.9 M and 2.0 M HNO₃. This decline in specificity is believed to be caused by the overall decrease in mother liquor volume after crystallization. As shown in Table 5, the percent volume decrease in the mother liquor with the 2.0 M HNO₃ system is significantly greater than that of 4.3 M HNO₃ system, ~30%. The reduction in volume slightly deviates from that calculated by Equation (2), with showing less volume reduction. This is believed to be caused by an increase in the amount of dissolved species in the supernate, which should increase the volume slightly.

Table 5: Selectivity at different initial acidities.

| Analyte | 4.3 M HNO ₃ | | 3.4 M HNO ₃ | | 2.9 M HNO ₃ | | 2.0 M HNO ₃ | |
|------------------|------------------------|-------|------------------------|-------|------------------------|-------|------------------------|-------|
| | %Removed | %U/%M | %Removed | %U/%M | %Removed | %U/%M | %Removed | %U/%M |
| Sr ²⁺ | <1% | >81 | 58% ± 3% | 1.3 | 70% ± 4% | 1.3 | 93% ± 5% | 1.0 |
| Cs ⁺ | <1% | >81 | <1% | >84 | 34% ± 2% | 2.6 | 32% ± 2% | 2.9 |
| Nd ³⁺ | <1% | >81 | <1% | >84 | 35% ± 2% | 2.5 | 31% ± 2% | 3.0 |
| U(VI) | 81% ± 5% | - | 84% ± 5% | - | 89% ± 5% | - | 95% ± 10% | - |
| %Vol | -55% | | -63% | | -72% | | -85% | |

The effect of NaBiO₃ on the selectivity was then studied and found to not only improve the selectivity of the An(VI) crystallization, but enhance the yield simultaneously. As mentioned earlier, NaBiO₃ has established itself as the benchmark for Am oxidation; therefore, it is important to understand what effects its presence will have on the separation and crystallization

as a whole. Table 6 displays the results of separations at 4.3 M and 3.4 M HNO₃ with the addition of roughly 121 mM and 115 mM NaBiO₃, respectively. The presence of BiO₃⁻ in solutions seems to increase the solubility limit of U(VI), allowing for a greater UNH yield upon cooling. The presence of BiO₃⁻ also seems to prevent the fission products from being removed from solution during crystallization, even at the lower acidity of 3.4 M HNO₃. While on a process level, it may not be practical to add large amounts of mass to the system to achieve the high oxidation potential needed to achieve Am(VI), from these results it appears to be advantageous, increasing the yield and selectivity.

Table 6: Selectivity in the presence of BiO₃⁻.

| Analyte | 4.3 M HNO ₃ | | 3.4 M HNO ₃ | |
|------------------|------------------------|-------|------------------------|-------|
| | %Removed | %U/%M | %Removed | %U/%M |
| Sr ²⁺ | <1% | >86 | <1% | >90 |
| Cs ⁺ | <1% | >86 | <1% | >90 |
| Nd ³⁺ | <1% | >86 | <1% | >90 |
| Bi | <1% | >86 | <1% | >90 |
| U(VI) | 86% ± 5% | - | 90% ± 5% | - |

Our previous work (Burns and Moyer, 2016) indicated that there might be some interactions between fission products, specifically, tetravalent ions, like Zr⁴⁺ and Ce⁴⁺, forming double nitrate salts with Cs⁺, as shown in Equation (3). This has also been observed in the JAEA NEXT process (Sano et al., 2007) with Pu⁴⁺. To understand the behavior of double nitrate complex formation, a system containing Cs, Zr, and U(VI) at concentration of 27 mM, 14 mM, and 3.5 M, respectively, with the initial acidity of 4.3 M HNO₃ was studied. Table 7 displays the results of the amount of metal removed from solution after cooling from 58 °C to 40 °C and 20 °C, resulting in neither Cs or Zr being removed from solution. These results indicate that the solubility limit of the double nitrate salt Cs₂Zr(NO₃)₆ is above 36 mM or the double nitrate complex is not forming in this system. In either case, this is a positive result, when considering that Zr is historically very difficult to deal with in a solvent extraction PUREX-type separation scheme, where it tends to follow the bulk of Pu through the process.



Table 7: Behavior of Cs⁺ and Zr⁴⁺ during crystallization of UNH

| Analyte | 40 °C | | 20 °C | |
|------------------|----------|-------|----------|-------|
| | %Removed | %U/%M | %Removed | %U/%M |
| Zr ⁴⁺ | <1% | >17 | <1% | >79 |
| Cs ⁺ | <1% | >17 | <1% | >79 |
| U(VI) | 17% ± 1% | - | 79% ± 4% | - |

Another system was studied at an initial acidity of 4.25 M HNO₃ containing Cs, Ce, and U(VI) at concentration of 29 mM, 14 mM, and 3.9 M, respectively. However, in order to achieve the tetravalent oxidation state of Ce⁴⁺, NaBiO₃ was added to the system as well. Table 8 displays the results of the amount of metal removed from solution after cooling from 58 °C to 40 °C and

20 °C, showing similar results as with the Cs and Zr system, with neither Cs or Ce being removed from solution. Again, it is not clear if the precursor to the double nitrate salt of $\text{Ce}(\text{NO}_3)_6^{2-}$ is forming, only that $\text{Cs}_2\text{Ce}(\text{NO}_3)_6$ is not precipitating out of solution.

Table 8: Behavior of Cs^+ and Zr^{4+} during crystallization of UNH

| Analyte | 40 °C | | 20 °C | |
|------------------|----------|-------|----------|-------|
| | %Removed | %U/%M | %Removed | %U/%M |
| Cs^+ | <1% | >27 | <1% | >83 |
| Ce^{4+} | <1% | >27 | <1% | >83 |
| Bi | <1% | >27 | <1% | >83 |
| U(VI) | 27% ±1% | - | 83% ± 5% | - |

4. Conclusions

Good yield and selectivity of a hexavalent actinide crystallization separation suggests an alternative approach to more traditional approaches using solvent extraction for recovery of actinides for nuclear fuel recycle. The solubility limit of UNH at a range of nitric acid concentrations and temperatures was determined, and the yield of UNH crystallization was calculated. The yield was found to increase with a decrease in the initial nitric acid concentration prior to cooling the saturated uranyl nitrate solution from 50 °C to 2 °C. A direct correlation in the decrease of solution volume percent and U mass percent removed from solution was observed. A slow cooling rate was shown to significantly increase selectivity for U(VI) over Sr, Cs, and Nd, as it facilitates a slow rate of UNH crystal formation, eliminating incorporation of defects. Higher acid concentrations of ca. 4.3 M HNO_3 were shown to produce a more selective separation, presumably caused by a smaller reduction in mother liquor volume in the higher acid systems. The addition of NaBiO_3 appeared to increase both yield and selectivity. Finally, there was no evidence of any precipitation of tetravalent metal double nitrate salts. These results taken together indicate that a hexavalent crystallization scheme offers a potentially simple approach to a complex problem of enormous potential benefit to sustainable energy, where a single separation technology is employed, crystallization, and a high-yield, high-purity product is generated.

Acknowledgements

This work was sponsored by the Fuel Cycle Research and Development program, Office of Nuclear Energy, U.S. Department of Energy, for which the authors are very grateful.

References

- Aneheim, E., Ekberg, C., Fermvik, A., Foreman, M.R.S.J., Retegan, T., Skarnemark, G., 2010. A TBP/BTBP-based GANEX Separation Process. Part 1: Feasibility. *Solvent Extr. Ion Exch.* 28, 437–458. doi:10.1080/07366299.2010.480930
- Ansari, S.A., Pathak, P., Mohapatra, P.K., Manchanda, V.K., 2011. Aqueous Partitioning of

- Minor Actinides by Different Processes. *Sep. Purif. Rev.* 40, 43–76.
doi:10.1080/15422119.2010.545466
- Burns, J.D., Borkowski, M., Clearfield, A., Reed, D.T., 2012a. Separation of oxidized americium from lanthanides by use of pillared metal(IV) phosphate-phosphonate hybrid materials. *Radiochim. Acta* 100, 901–906. doi:10.1524/ract.2013.1990
- Burns, J.D., Clearfield, A., Borkowski, M., Reed, D.T., 2012b. Pillared metal(IV) phosphate-phosphonate extraction of actinides. *Radiochim. Acta* 100, 381–387.
doi:10.1524/ract.2012.1929
- Burns, J.D., Moyer, B.A., 2016. Group Hexavalent Actinide Separations: A New Approach to Used Nuclear Fuel Recycling. *Inorg. Chem.* 55, 8913–8919.
doi:10.1021/acs.inorgchem.6b01430
- Burns, J.D., Shehee, T.C., Clearfield, A., Hobbs, D.T., 2012c. Separation of Americium from Curium by Oxidation and Ion Exchange. *Anal. Chem.* 84, 6930–6932.
doi:10.1021/ac3018394
- Dares, C.J., Lapidés, A.M., Mincher, B.J., Meyer, T.J., 2015. Electrochemical oxidation of ²⁴³Am(III) in nitric acid by a terpyridyl-derivatized electrode. *Science* 350, 652–655.
doi:10.1126/science.aac9217
- Grimes, R.W., Nuttall, W.J., 2010. Generating the Option of a Two-Stage Nuclear Renaissance. *Science* 329, 799–803. doi:10.1126/science.1188928
- Grimes, T.S., Mincher, B.J., 2015. Effect of solvent extraction processes on Am(VI) reduction kinetics, in: 250th ACS National Meeting & Exposition. Boston.
- Haynes, W.M. (Ed.), 2016. *CRC Handbook of Chemistry and Physics*, 97th ed. CRC Press, Boca Raton, FL.
- Kharecha, P.A., Hansen, J.E., 2013. Prevented mortality and greenhouse gas emissions from historical and projected nuclear power. *Environ. Sci. Technol.* 47, 4889–95.
doi:10.1021/es3051197
- Manchanda, V., Pathak, P., Mohapatra, P., 2009. New Developments in Thorium, Uranium, and Plutonium Extraction, in: Moyer, B.A. (Ed.), *Ion Exchange and Solvent Extraction A Series of Advances*, Volume 19. CRC Press, Philadelphia, pp. 65–118.
doi:10.1201/9781420059700-c2
- Miguirditchian, M., Chareyre, L., Heres, X., Hill, C., Baron, P., Masson, M., 2007. GANEX: Adaptation of the DIAMEX-SANEX Process for the Group Actinide Separation, in: *GLOBAL 2007*. American Nuclear Society, La Grange Park, IL, pp. 550–552.
- Mincher, B.J., Martin, L.R., Schmitt, N.C., 2012. Diamylmethylphosphonate Solvent Extraction of Am(VI) from Nuclear Fuel Raffinate Simulant Solution. *Solvent Extr. Ion Exch.* 30, 445–456. doi:10.1080/07366299.2012.671108
- Mincher, B.J., Martin, L.R., Schmitt, N.C., 2008. Tributylphosphate Extraction Behavior of Bismuthate-Oxidized Americium. *Inorg. Chem.* 47, 6984–6989. doi:10.1021/ic800667h
- Mincher, B.J., Schmitt, N.C., Schuetz, B.K., Shehee, T.C., Hobbs, D.T., 2015a. Recent advances

- in f-element separations based on a new method for the production of pentavalent americium in acidic solution. *RSC Adv.* 5, 27205–27210. doi:10.1039/C5RA03196F
- Mincher, B.J., Tillotson, R.D., Garn, T., Rutledge, V., Law, J., Schmitt, N.C., 2015b. The solvent extraction of Am(VI) using centrifugal contactors. *J. Radioanal. Nucl. Chem.* doi:10.1007/s10967-015-4397-6
- Moyer, B.A., Lumetta, G.J., Mincher, B.J., 2015. Minor actinide separation in the reprocessing of spent nuclear fuels: recent advances in the United States, in: *Reprocessing and Recycling of Spent Nuclear Fuel*. Woodhead, Cambridge, pp. 289–312. doi:10.1016/B978-1-78242-212-9.00011-3
- Nakahara, M., Kaji, N., Yano, K., Shibata, A., Takeuchi, M., Okano, M., Kuno, T., 2013. Nitric Acid Concentration Dependence of Dicesium Plutonium(IV) Nitrate Formation during Solution Growth of Uranyl Nitrate Hexahydrate. *J. Chem. Eng. JAPAN* 46, 56–62. doi:10.1252/jcej.12we175
- Nuclear Fuel Recovery and Recycling Center. License application, PSAR, volume 7, 1976. . Richland.
- Poinssot, C., Boullis, B., Bourg, S., 2015. Reprocessing and Recycling of Spent Nuclear Fuel, in: *Reprocessing and Recycling of Spent Nuclear Fuel*. Woodhead, Cambridge, pp. 27–48. doi:10.1016/B978-1-78242-212-9.00002-2
- Runde, W.H., Mincher, B.J., 2011. Higher Oxidation States of Americium: Preparation, Characterization and Use for Separations. *Chem. Rev.* 111, 5723–5741. doi:10.1021/cr100181f
- Sailor, W.C., 2000. NUCLEAR POWER: A Nuclear Solution to Climate Change? *Science* 288, 1177–1178. doi:10.1126/science.288.5469.1177
- Salvatores, M., Palmiotti, G., 2011. Radioactive waste partitioning and transmutation within advanced fuel cycles: Achievements and challenges. *Prog. Part. Nucl. Phys.* 66, 144–166. doi:10.1016/j.pnpnp.2010.10.001
- Sano, Y., Miura, S., Nakahara, M., Kamiya, M., Nomura, K., Komaki, J., 2007. Plutonium and other actinides behaviour in NEXT process. *J. Alloys Compd.* 444–445, 397–403. doi:10.1016/j.jallcom.2007.03.092
- Tachimori, S., Morita, Y., 2009. Overview of Solvent Extraction Chemistry for Reprocessing., in: Moyer, B.A. (Ed.), *Ion Exchange and Solvent Extraction A Series of Advances, Volume 19*. CRC Press, Philadelphia, pp. 1–63. doi:10.1201/9781420059700-c1
- Todd, T.A., Wigeland, R.A., 2006. Advanced Separation Technologies for Processing Spent Nuclear Fuel and the Potential Benefits to a Geologic Repository, in: Lumetta, G.J., Nash, K.L., Clark, S.B., Friese, J.I. (Eds.), *Separations for the Nuclear Fuel Cycle in the 21 St Century*, ACS Symposium Series. American Chemical Society, Washington, DC, pp. 41–55. doi:10.1021/bk-2006-0933
- Wigeland, R.A., Taiwo, T., Todosow, M., 2015. Investigation of Benefits from U/TRU Recycle - Quantification and Comparison to U/Pu Recycle, in: *Global 2015*. Paris, France, pp. 329–335.

Wigeland, R., Bauer, T., Fanning, T., Morris, E., 2006. Separations and transmutation criteria to improve utilization of a geologic repository. Nucl. Technol. 154, 95–106.

